FEBS Letters 587 (2013) 2512–2516

journal homepage: www.FEBSLetters.org

The [NiFe]-hydrogenase accessory chaperones HypC and HybG of *Escherichia coli* are iron- and carbon dioxide-binding proteins

Basem Soboh [a,1], Sven T. Stripp [b,1], Claudia Bielak [a], Ute Lindenstrauß [a], Mario Braussemann [a], Mahwish Javaid [a], Magnus Hallensleben [a], Claudia Granich [a], Martin Herzberg [a], Joachim Heberle [b], R. Gary Sawers [a,*]

[a] Institute of Microbiology, Martin-Luther University Halle-Wittenberg, Kurt-Mothes-Str. 3, 06120 Halle (Saale), Germany
[b] Freie Universität Berlin, Experimental Molecular Biophysics, Arnimalle 14, 14195 Berlin, Germany

ARTICLE INFO

Article history:
Received 5 June 2013
Revised 27 June 2013
Accepted 27 June 2013
Available online 10 July 2013

Edited by Peter Brzezinski

Keywords:
Carbon dioxide
Hydrogenase
Iron
Infrared spectroscopy
Metalloprotein
Maturation

ABSTRACT

[NiFe]-hydrogenase accessory proteins HypC and HypD form a complex that binds a Fe–$(CN)_2CO$ moiety and CO_2. In this study two HypC homologues from *Escherichia coli* were purified under strictly anaerobic conditions and both contained sub-stoichiometric amounts of iron (approx. 0.3 mol Fe/mol HypC). Infrared spectroscopic analysis identified a signature at 2337 cm^{-1} indicating bound CO_2. Aerobically isolated HypC lacked both Fe and CO_2. Exchange of either of the highly conserved amino acid residues Cys2 or His51 abolished both Fe- and CO_2-binding. Our results suggest that HypC delivers CO_2 bound directly to Fe for reduction to CO by HypD.

Structured summary of protein interactions:
HypC and **HypC** bind by comigration in sds page (View interaction)
HybG and **HybG** bind by comigration in sds page (View interaction)

1. Introduction

[NiFe]-hydrogenases catalyze both H_2 evolution as well as H_2 oxidation [1]. The catalytic subunit of the enzyme harbours a NiFe–$(CN)_2CO$ cofactor and its synthesis requires the coordinated activities of a number of highly conserved Hyp accessory proteins [2,3]. The cyanide ligands (CN^-) are derived from carbamoylphosphate [4,5], while the metabolic origin of the carbonyl ligand (CO) is still unresolved.

Recent studies have revealed that biosynthesis of the Fe–$(CN)_2$-CO moiety is likely to occur on an assembly platform comprising minimally the HypC, HypD and HypE proteins, with HypD forming the key scaffold [6–8]. Fourier-transform infrared (FT-IR) analysis of an anaerobically isolated complex of HypC and HypD (HypCD) revealed signatures for CO and two CN^- ligands [6,7]. Moreover, an additional contribution at 2337 cm^{-1} was identified, which is consistent with the asymmetrical stretch vibration of CO_2 [6]. The peak is characteristic of bound CO_2 and can be clearly distinguished from CO_2 dissolved in water (2342 cm^{-1}) and gaseous (2349 cm^{-1}) CO_2 [9,10].

Once the Fe–$(CN)_2CO$ group is synthesized, it is proposed that the moiety is transferred by HypC to a precursor form of the hydrogenase large subunit [3,11]. This proposition is based on the fact that as well as forming a complex with HypD [11,12], HypC also has been isolated in complex with the hydrogenase large subunit [13]. The combined results of these studies have led to a formulation of the HypC cycle in which the 10 kDa protein acts as a chaperone shuttling between the iron–sulfur protein HypD and the hydrogenase large subunit apo-protein [11].

The HypC/HupF superfamily comprises proteins of approximately 90 amino acid residues [14–16]. Early mutagenesis studies revealed that HypC has a highly conserved cysteinyl residue at amino acid position 2, which is essential for complex formation with HypD and for maturation activity [11,17]. The crystal structure of HypC [18] revealed that this N-terminal cysteinyl residue is located in an OB-fold and is in proximity to a conserved histidine residue (His51 in *Escherichia coli*). It has been suggested that these two residues coordinate the iron ion of the Fe–$(CN)_2CO$ cofactor [19].

Many organisms that synthesize multiple hydrogenases have more than one HypC homolog, e.g., *E. coli* synthesizes the homologs

* Corresponding author. Fax: +49 345 5527010.
E-mail address: gary.sawers@mikrobiologie.uni-halle.de (R.G. Sawers).
[1] These authors contributed equally to this work.

0014-5793/$36.00
http://dx.doi.org/10.1016/j.febslet.2013.06.055

HypC and HybG [20]. Mutants lacking *hypC* fail to complete hydrogenase 3 (Hyd-3) maturation and consequently lack an active hydrogen-evolving formate hydrogenlyase (FHL) complex [2,20]. The *hybG* gene, in contrast, is located within the *hyb* operon encoding both structural and accessory components of Hyd-2 [21]; HybG is required for biosynthesis of both Hyd-1 and Hyd-2, and interacts with both apo-large subunits [20,22].

The combined action of the carbamoyl transferase HypF and the ATP-dependent dehydratase HypE supplies the cyanyl ligands and HypD is the enzyme that assembles the Fe–$(CN)_2CO$ moiety [8]. The metabolic origin and route of delivery of the carbonyl ligand are both unclear. Moreover, little is known about how the iron ion in the Fe–$(CN)_2CO$ moiety is supplied to HypD, as recent evidence suggests that the route is independent of the FeS biosynthetic machinery [23]. Here we present evidence that the HypC superfamily represents a new class of Fe- and CO_2-binding proteins, suggesting that HypC delivers Fe along with CO_2 to the redox-active HypD scaffold protein where reduction to CO probably takes place.

2. Materials and methods

2.1. Bacterial strains, plasmids and growth conditions

The *E. coli* strains used included MC4100 [24], DHB-G (Δ*hybG*) [20], DHP-C (Δ*hypC*) [2], BEF314 (Δ*hypB-E*) [2], DHP-H2 (Δ*hypF*) [25] and BL21(DE3) [26]. The plasmids used included phypDHis [8], pT-hypDEFCStrep [12], pASK-hybG encoding C-terminally Strep-tagged $HybG_{Strep}$, pT-hypC plasmid coding for $HypC_{Strep}$, phypCHis and pHishypC, encoding C- and N-terminally His-tagged HypC, respectively and phybGHis encoding $HybG_{His}$. The *hybG* gene was amplified from the chromosome of MC4100 using appropriately designed oligonucleotides (Table S1) and the PCR product was subsequently digested with BsaI and ligated into the BsaI restriction site of pASK-IBA3 (IBA, Göttingen, Germany), to generate pASK-hybG encoding $HybG_{Strep}$. Restriction digestion of pT-hypDC [12] with NdeI removed the *hypD* gene and re-ligation of the plasmid backbone delivered plasmid pT-hypC coding for $HypC_{Strep}$. Plasmid pT-hypC was used as template for site-directed mutagenesis of the *hypC* gene (QuikChange procedure of Stratagene) and the oligonucleotide primers are listed in Table S1.

To construct plasmids coding for N-terminally His-tagged $_{His}$HypC protein, chromosomal DNA from MC4100 was used as the template for PCR-amplification of *hypC* (primers listed in Table S1) and it was ligated into NdeI-/HindIII-digested pET28A (Novagen) to generate the plasmid phypC. To generate plasmids coding for C-terminally His-tagged $HypC_{His}$ and $HybG_{His}$, EcoRI- and HindIII-digested pET30 (Novagen) was used and the resulting DNA fragments carrying the complete *hypC* or *hybG* genes were ligated into pET30 to generate the plasmids phypCHis and phybG-His, respectively.

E. coli strain BL21(DE3) transformed with the appropriate plasmid was grown in modified TB medium [6], containing 100 μg $ml^{-1}$of ampicillin or 50 μg ml^{-1} kanamycin as appropriate at 37 °C on a rotary shaker until an optical density of 0.4 at 600 nm was reached. Gene expression was induced by the addition of either 0.3 mM IPTG or 0.2 μg ml^{-1} anhydrotetracyclin followed by incubation at 30 °C for 3–5 h. Cells were harvested (OD_{600nm} of 1.0) by centrifugation for 30 min at 50000×*g* at 4 °C and cell pellets were used either immediately or stored at −20 °C until use.

2.2. Protein purification

Unless stated otherwise, all steps were carried out under anaerobic conditions in an anaerobic chamber (Coy Laboratories, Grass Lake, USA). His-tagged and Strep-tagged proteins and protein complexes were purified exactly as described previously [6,8].

2.3. FTIR spectroscopy

Fourier-transform infrared (FT-IR) spectroscopy was performed exactly as described [8] using on a Tensor27 (Bruker Optik, Ettlingen, Germany) equipped with a three-reflection silicon crystal attenuated total reflection (ATR) cell (Smith Detection, Warrington, USA). Protein samples (typically 1 μl of 10 mg ml^{-1} HypC or HybG) were dried on top of the ATR crystal under pure N_2 or air by help of home made gas mixers. HybG isolated from BEF314 (Δ*hypBCDE*) was probed on a one-reflection germanium ATR cell (Pike Technologies, Madison, USA). To extract Fe ions from HybG, samples were incubated with up to 20 mM EDTA in buffer W for 5 min prior to ATR analysis of the mixture. Oxidation of HypC or HybG by H_2O_2 was performed on wetted films [8]. All spectra were recorded at room temperature.

2.4. Non-heme Fe determination

Iron content was determined by inductively coupled plasma mass spectrometry (ICP-MS) exactly as described [6]. For ICP-MS analysis 0.1 mg of purified HypC or HybG (1 mg ml^{-1}) was used and samples were analyzed for iron, nickel, zinc, and copper.

2.5. Other methods

SDS–PAGE was performed using 15% (w/v) polyacrylamide as described [27] and polypeptides were transferred to nitrocellulose membranes as described [28]. Determination of protein concentration was done as described [29].

UV–vis spectroscopy was performed as described [6]. The protein concentration of HypC or HybG variants was 5 mg ml^{-1}.

3. Results and discussion

3.1. Oxygen-labile coordination of Fe by HypC and HybG

The $HypC_{His}$ protein was readily purified from crude extracts of BL21(DE3) and migrated as an approximately 10 kDa polypeptide in SDS–PAGE (Fig. 1A). If cell disruption and affinity chromatographic steps on Co^{2+}–NTA Sepharose were performed aerobically, enriched $HypC_{His}$ was colorless and had no associated cofactors. If oxygen was excluded from all steps, however, the resulting HypC protein was brown in color. The Fe content of purified $HypC_{His}$ was determined by inductively coupled plasma-emission mass spectrometry (ICP-MS) to be 0.32 ± 0.08 mol Fe per mol protein. To rule out that Fe was non-specifically bound to the C-terminal His-tag, a version of HypC was constructed with a Strep-tag in the same position. After over-production in BL21(DE3) and anaerobic isolation on Streptactin–Sepharose $HypC_{Strep}$ had on average 0.31 ± 0.06 mol Fe associated with the protein. Isolation of the tagged proteins in air resulted in a ten-fold decrease in Fe concentration (<0.03 mol).

Fusion of the His-tag with Cys2 at the N-terminus of HypC resulted in a protein that failed to restore hydrogenase 3 activity to an *E. coli hypC* mutant (not shown) and when isolated by anaerobic purification, $_{His}$HypC was essentially colorless and devoid of Fe (<0.01 mol) as determined by ICP-MS. This result indicated that, despite the Cys residue being present, no stable Fe bound to the protein presumably because the amino terminus of the cysteinyl residue was blocked by the His-tag.

To determine whether Fe-binding was a general feature of HypC proteins, we isolated both C-terminally His- and Strep-tagged

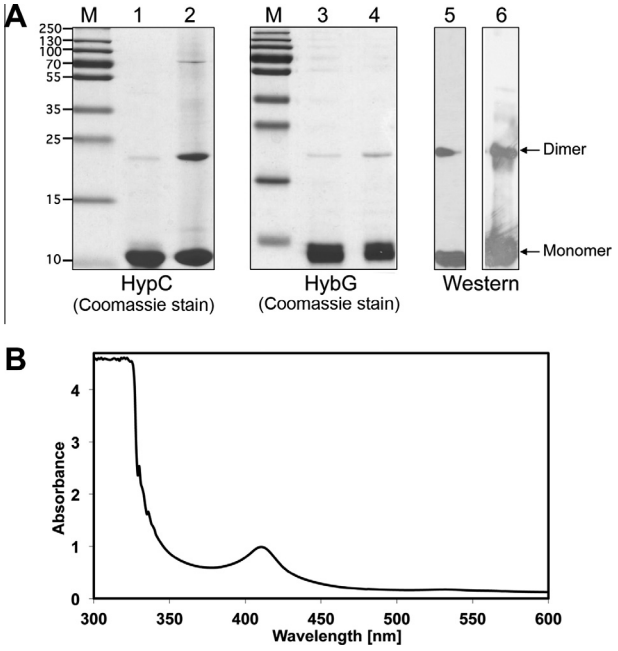

Fig. 1. Biochemical analysis of HybG and HypC. (A) Purified HybG and HypC variants (5 μg of each) were separated by SDS–polyacrylamide gel electrophoresis (15% w/v polyacrylamide) and subsequently stained with Coomassie Brilliant Blue (lanes 1 through 4) or transferred to a nitrocellulose membrane and challenged with anti-His-tag antiserum (lane 5) or anti-Strep antiserum (lane 6). Both sets of antibodies were used at a dilution of 1:3000. The position of a HypC and HybG dimer species is indicated. Dimer formation after SDS–PAGE was unaffected by oxygen. Lanes: M, PageRuler prestained marker in kDa (Fermentas #SM1811/2); 1, $HypC_{His}$; lane 2, $HypC_{strep}$; lane 3, $HybG_{His}$; lane 4, $HybG_{Strep}$; lane 5, $HypC_{His}$ (2 μg); lane 6, $HybG_{Strep}$ (2 μg). (B) UV–vis absorption spectrum of anaerobically purified $HybG_{Strep}$ (5 mg ml^{-1}).

variants of the *E. coli* HypC homolog, HybG (Fig. 1A). It was noted that purified $HybG_{Strep}$ revealed both a 10 kDa and a 20 kDa polypeptide upon SDS–PAGE analysis (Fig. 1A). Western blot analysis with anti-Strep antiserum confirmed that the 20 kDa band contains Strep-tagged polypeptide and mass spectrometry identified the band as HybG. A similar observation was made for $HypC_{His}$, suggesting that both HypC and HybG are capable of forming minimally homodimers; however, why they were resistant to denaturation in SDS buffer remains to be resolved. Attempts to determine the oligomeric state of HypC or HybG by anaerobic gel filtration or native PAGE revealed no discrete peak but only multiple oligomeric species suggesting that native HypC readily forms higher-order structures.

Metal analysis revealed a similar Fe ratio for $HybG_{His}$ and $HybG_{Strep}$ (0.3 ± 0.01 mol Fe/mol protein and 0.34 ± 0.01 mol Fe/mol protein, respectively). UV–visible spectroscopy of $HybG_{Strep}$ revealed an absorbance peak at 420 nm (Fig. 1B). Together, these findings suggest that HypC might supply the Fe ion for biosynthesis of the Fe–$(CN)_2CO$ moiety. This finding would be consistent with recent results [23], which indicate that the Fe ion for cofactor biosynthesis is not supplied by the Isc or Suf iron–sulfur cluster biogenesis pathways.

3.2. Anaerobically isolated HypC and HybG reveal FT-IR signatures of bound CO_2

Recent studies revealed that in addition to absorption bands at 2095 cm^{-1}, 2073 cm^{-1} and 1955 cm^{-1} characteristic of metal-bound CO and CN^- ligands the anaerobically isolated HypCD complex also exhibited a signature at 2337 cm^{-1}, which was assigned to the asymmetrical stretch vibration (ν_3) of CO_2 [6] (see also

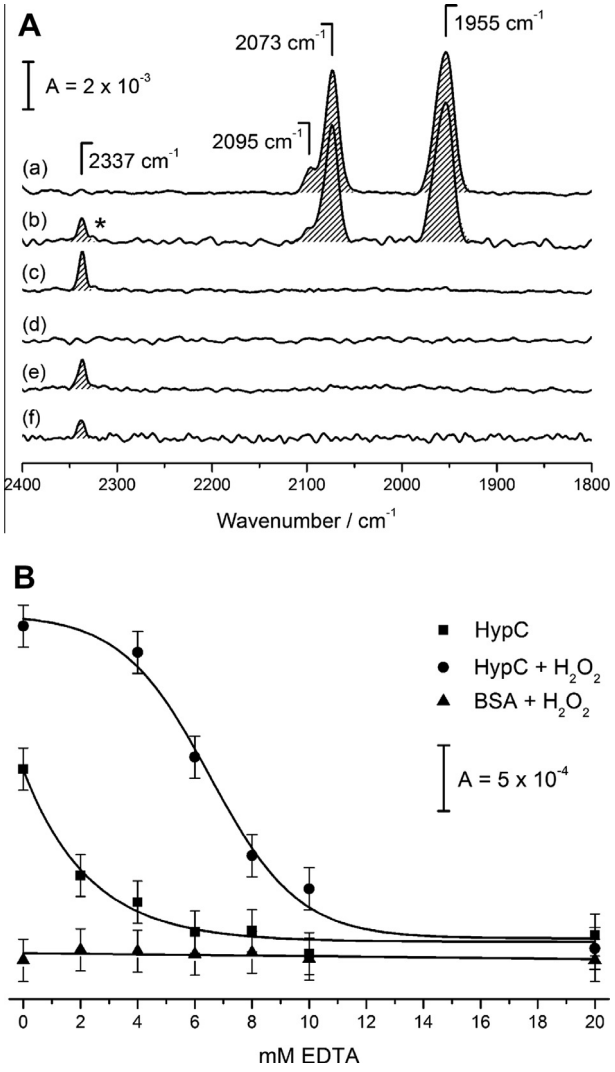

Fig. 2. FT-IR analysis of HypC and HybG variants and HypD complexes. (A) All samples were dried under N_2 and probed via ATR FT-IR in the absence of O_2. The displayed spectra are the average of 4096 scans recorded at a spectral resolution of 4 cm^{-1}. For the spectrum shown in (f) 30720 spectra were averaged. Water absorption was subtracted by a broad spline function. Spectra are scaled to amide II band height. Spectra: (a) HypD with bands fit to 1955 cm^{-1} (CO), 2073 cm^{-1} (CN^1), and 2095 cm^{-1} (CN^2); (b) HypCD complex with bands fit to 2324 cm^{-1} (hot-band as indicated by *) and 2337 cm^{-1} (ν_3 of CO_2); (c) $HypC_{His}$; (d) $_{His}$HypC; (e) $HybG_{His}$; (f) HypC_dBCDE. (B) FT-IR analysis of 'natural' CO_2 in $HybG_{His}$ as a function of EDTA concentration (squares). The 2337 cm^{-1} peak height is plotted and fits exponentially with $R = 0.97$. Circles represent the intensity of the 2337 cm^{-1} peak in $HybG_{His}$ samples treated with 1% (v/v) H_2O_2. This serves as a measure of Fe concentration and is plotted against cEDTA (sigmoidal fit with $R = 0.98$). Both Fe and CO_2 are lost upon increasing the EDTA concentration. BSA serves as a negative control (triangles).

Fig. 2A, spectrum b). Purified HypD shows signatures of CO and CN^- exclusively [8] (see Fig. 2A, spectrum a). Infrared analysis of anaerobically isolated HypC and HybG revealed no signatures in the CO/CN^- region; however, a sharp peak at 2337 cm^{-1} was detected (Fig. 2A, spectra c and e). As expected for CO_2 binding [30], a minor contribution could be fitted to the shoulder at 2326 cm^{-1} (mainly visible in Fig. 2A, spectra b and c). Both signatures were absent in aerobically isolated HypC and HybG proteins (not shown) and they were also not detected in N-terminally tagged $_{His}$HypC (Fig. 2A, spectrum d).

To rule out that HypD, or any of the other Hyp accessory proteins, was required for iron- and CO_2– binding $HybG_{Strep}$ was purified anaerobically from strain BEF314 (Δ*hypB-E*) [2]. The protein

had an iron content of approximately 0.3 (determined with two independent preparations) and it revealed a sharp peak at 2337 cm^{-1} (Fig. 2A, spectrum f). Similar results were obtained when $HybG_{Strep}$ was purified from DHP-F2 (Δ*hypF*) (data not shown).

3.3. Cys2Ala and His51Arg variants do not show the CO_2 signature

A Cys2Ala variant of $HypC_{Strep}$ lacked iron (<0.01 mol Fe) and FT-IR analysis of the anaerobically isolated protein showed no absorbance band at 2337 cm^{-1} (spectrum similar to d in Fig. 2A). Similarly, a His51Arg variant of $HypC_{His}$ also lacked the absorption band at the 2337 cm^{-1} wavenumber (not shown) and ICP-MS analysis showed that His51Arg-substituted $HypC_{Strep}$ does not bind iron (<0.01 mol Fe). In a previous study it was reported that a His51Arg variant of HypC lacked hydrogen gas production [31]. Together, these data indicate that Cys2 and His51 are required for coordination of both Fe and CO_2.

3.4. Strong correlation between Fe- and CO_2-binding suggested from reactions with EDTA and H_2O_2

Treatment of either $HypC_{Strep}$ or $HybG_{His}$ with EDTA resulted in concomitant loss of bound Fe and the CO_2 signature at 2337 cm^{-1}. To probe the loss of Fe spectroscopically, samples of $HybG_{His}$ were treated with up to 20 mM EDTA and a H_2O_2/water vapor mixture as reported earlier [8]. In a process commonly referred to as Fenton chemistry, H_2O_2 is reduced by Fe^{2+} to produce OH^- radicals, which rapidly oxidize the amino acid environment of the metal site [32]. The CO_2 released in this reaction is detected as a transient off-gas unspecifically bound to the protein film [33,34]. A new peak forms at 2337 cm^{-1} whose height is a direct measure of Fe^{2+} concentration. As the ν_3 mode is vibrationally insensitive to the ligand of CO_2 [10,35], 'natural' and Fenton CO_2 both appear at the same position. It is important to note that CO_2 was detected in as-isolated samples only under strictly reducing conditions. Thus, contamination of the natural signal with Fenton CO_2 is highly unlikely. Fig. 2B shows the decrease of Fenton CO_2 (circles) as a function of EDTA concentration in comparison to the loss of 'natural' CO_2 (squares) in as-isolated $HybG_{His}$. Both natural and Fenton-generated CO_2 were sequentially measured on the same sample. Bovine serum albumin (BSA, triangles) was used as a negative control to ensure that the CO_2 released in the H_2O_2 assay depended exclusively on Fe and was not directly affected by incubation with EDTA. The bending mode of gaseous CO_2 in the far-IR (667 cm^{-1}) is more suitable to analyze the chemical nature of the binding partner [10,36]; however, we failed to detect the ν_2 absorption band in HypC and HybG due to low signal intensity.

Together, these results are consistent with the proposal [37] that metabolic CO_2 could be the origin of the CO ligand. This is also in accord with ^{13}C-labeling studies in which exogenously supplied CO_2 failed to result in a red-shift in the absorption band of CO at 1955 cm^{-1} [38]. Despite being highly characteristic, the asymmetric stretch vibration of CO_2 is not informative with regard to ligation partners. Mascetti and Tranquille reported that CO_2 binds to transition metals like Fe via the carbon atom, leaving the ν_3 vibration largely unaffected [35]. Both the observation of a concerted loss of Fe and CO_2 upon EDTA treatment plus the precise overlap of natural and Fenton CO_2 at 2337 cm^{-1} in Fig. 2B supports this coordination model.

4. Conclusions

The findings presented in this study demonstrate that HypC/HybG binds both Fe and CO_2 and this is independent of the other Hyp accessory proteins. Residues Cys2 and His51 of HypC are both essential for binding of CO_2 and Fe. Together with our recent demonstration that HypD is the scaffold on which the Fe–$(CN)_2CO$ moiety is assembled [8], the findings presented here strongly suggest that HypC proteins deliver an Fe with bound CO_2 to the redox-active HypD where reduction to CO occurs. Future studies will be required to prove that both the Fe ion and CO_2 attached to HypC are the direct precursors of the Fe–$(CN)_2CO$ moiety.

Acknowledgements

The authors are indebted to Denise Hübner for help with protein purification and to Chris Pickett and Wolfgang Weigand for discussion. The work conducted in the authors' laboratories was supported by EFRE funds of the EU and the DFG (Grant SA 494/3–1, 494/3–2) to R.G.S. and by the BMBF (H_2 design cells) to J.H.

Appendix A. Supplementary data

Supplementary data associated with this article can be found, in the online version, at http://dx.doi.org/10.1016/j.febslet.2013.06.055.

References

[1] Vignais, P.M. and Billoud, B. (2007) Occurrence, classification, and biological function of hydrogenases: an overview. Chem. Rev. 107, 4206–4272.
[2] Jacobi, A., Rossmann, R. and Böck, A. (1992) The *hyp* operon gene products are required for the maturation of catalytically active hydrogenase isoenzymes in *Escherichia coli*. Arch. Microbiol. 158, 444–451.
[3] Böck, A., King, P.W., Blokesch, M. and Posewitz, M.C. (2006) Maturation of hydrogenases. Adv. Microbiol. Physiol. 51, 1–71.
[4] Paschos, A., Glass, R.S. and Böck, A. (2001) Carbamoylphosphate requirement for synthesis of the active center of [NiFe]-hydrogenases. FEBS Lett. 488, 9–12.
[5] Reissmann, S., Hochleitner, E., Wang, H., Paschos, A., Lottspeich, F., Glass, R.S. and Böck, A. (2003) Taming of a poison: biosynthesis of the NiFe-hydrogenase cyanide ligands. Science 299, 1067–1070.
[6] Soboh, B., Stripp, S.T., Muhr, E., Granich, C., Braussemann, M., Herzberg, M., Heberle, J. and Sawers, R.G. (2012) [NiFe]-hydrogenase maturation: isolation of a HypC–HypD complex carrying diatomic CO and CN- ligands. FEBS Lett. 586, 3882–3887.
[7] Bürstel, I., Siebert, E., Winter, G., Hummel, P., Zebger, I., Friedrich, B. and Lenz, O. (2012) A universal scaffold for synthesis of the $Fe(CN)_2(CO)$ moiety of [NiFe] hydrogenase. J. Biol. Chem. 287, 38845–38853.
[8] Stripp, S.T., Soboh, B., Lindenstrauss, U., Braussemann, M., Herzberg, M., Nies, D.H., Sawers, R.G. and Heberle, J. (2013) HypD is the scaffold protein for Fe–(CN)2CO cofactor assembly in [NiFe]-hydrogenase maturation. Biochemistry 52, 3289–3296.
[9] Falk, M. and Miller, A.G. (1992) Infrared spectrum of carbon dioxide in aqueous solution. Vib. Spectrosc. 4, 105–108.
[10] Dobrowolski, J.C. and Jamróz, M.H. (1992) Infrared evidence for CO_2 electron donor-acceptor complexes. J. Mol. Struct. 275, 211–219.
[11] Blokesch, M. and Böck, A. (2002) Maturation of [NiFe]-hydrogenases in *Escherichia coli*: the HypC cycle. J. Mol. Biol. 324, 287–296.
[12] Blokesch, M., Albracht, S.P.J., Matzanke, B.F., Drapal, N.M., Jacobi, A. and Böck, A. (2004) The complex between hydrogenase-maturation proteins HypC and HypD is an intermediate in the supply of cyanide to the active site iron of [NiFe]-hydrogenases. J. Mol. Biol. 344, 155–167.
[13] Drapal, N. and Böck, A. (1998) Interaction of the hydrogenase accessory protein HypC with HycE, the large subunit of *Escherichia coli* hydrogenase 3 during enzyme maturation. Biochemistry 37, 2941–2948.
[14] Lutz, S., Jacobi, A., Schlensog, V., Böhm, R., Sawers, G. and Böck, A. (1991) Molecular characterization of an operon (*hyp*) necessary for the activity of the three hydrogenase isoenzymes in *Escherichia coli*. Mol. Microbiol. 5, 123–135.
[15] Dernedde, J., Eitinger, T., Patenge, N. and Friedrich, B. (1996) *Hyp* gene products in *Alcaligenes eutrophus* are part of a hydrogenase-maturation system. Eur. J. Biochem. 235, 351–358.
[16] Takács, M., Rákhely, G. and Kovács, K.L. (2001) Molecular characterization and heterologous expression of *hypCD*, the first two [NiFe]-hydrogenase accessory genes of *Thermococcus litoralis*. Arch. Microbiol. 176, 231–235.
[17] Magalon, A. and Bock, A. (2000) Analysis of the HypC–HycE complex, a key intermediate in the assembly of the metal center of the *Escherichia coli* hydrogenase 3. J. Biol. Chem. 275, 21114–21120.
[18] Watanabe, S., Matsumi, R., Arai, T., Atomi, H., Imanaka, T. and Miki, K. (2007) Crystal structures of [NiFe] hydrogenase maturation proteins HypC, HypD and HypE: insights into cyanation reaction by thiol redox signaling. Mol. Cell 27, 29–40.

[19] Watanabe, S., Matsumi, R., Atomi, H., Imanaka, T. and Miki, K. (2012) Crystal structures of the HypCD complex and the HypCDE ternary complex: transient intermediate complexes during [NiFe] hydrogenase maturation. Structure 20, 2124–2137.
[20] Blokesch, M., Magalon, A. and Böck, A. (2001) Interplay between the specific chaperone-like proteins HybG and HypC in maturation of hydrogenases 1, 2, and 3 from *Escherichia coli*. J. Bacteriol. 183, 2817–2822.
[21] Menon, N.K., Chatelus, C.Y., Dervartanian, M., Wendt, J.C., Shanmugam, K.T., Peck Jr., H.D. and Przybyla, A.E. (1994) Cloning, sequencing, and mutational analysis of the *hyb* operon encoding *Escherichia coli* hydrogenase 2. J. Bacteriol. 176, 4416–4423.
[22] Butland, G., Zhang, J.W., Yang, W., Sheung, A., Wong, P., Greenblatt, J.F., Emili, A. and Zamble, D.B. (2006) Interactions of the *Escherichia coli* hydrogenase biosynthetic proteins: HybG complex formation. FEBS Lett. 580, 677–681.
[23] Pinske, C. and Sawers, R.G. (2012) Delivery of iron-sulfur clusters to the hydrogen-oxidizing [NiFe]-hydrogenases in *Escherichia coli* requires the A-type carrier proteins ErpA and IscA. PLoS ONE 7, e31755.
[24] Casadaban, M.J. (1976) Transposition and fusion of the *lac* genes to selected promoters in *Escherichia coli* using bacteriophage lambda and Mu. J. Mol. Biol. 104, 541–555.
[25] Paschos, A., Bauer, A., Zimmermann, A., Zehelein, E. and Böck, A. (2002) HypF, a carbamoyl phosphate-converting enzyme involved in [NiFe] hydrogenase maturation. J. Biol. Chem. 277, 49945–49951.
[26] Studier, F.W. and Moffatt, B.A. (1986) Use of bacteriophage T7 RNA polymerase to direct selective high-level expression of cloned genes. J. Mol. Biol. 189, 113–130.
[27] Laemmli, U.K. (1970) Cleavage of structural proteins during the assembly of the head of bacteriophage T4. Nature 227, 680–685.
[28] Towbin, H., Staehelin, T. and Gordon, J. (1979) Electrophoretic transfer of proteins from polyacrylamide gels to nitrocellulose sheets: procedure and some applications. Proc. Natl. Acad. Sci. USA 76, 4350–4354.
[29] Lowry, O.H., Rosebrough, N.J., Farr, A.L. and Randall, R.J. (1951) Protein measurement with the Folin phenol reagent. J. Biol. Chem. 193, 265–275.
[30] Cunliffe-Jones, D.B. (1969) Perturbation of some vibrational bands in solution. Spectrochim. Acta 25A, 779–791.
[31] Blokesch, M. (2004) [NiFe]-Hydrogenasen von *Escherichia coli*: Funktionen der am Metalleinbau beteiligten Proteine. Ph.D. thesis, Ludwig–Maximilians University Munich.
[32] Stadtman, E.R. and Berlett, B.S. (1991) Fenton chemistry: amino acid oxidation. J. Biol. Chem. 266, 17201–17211.
[33] Cundari, T.R., Wilson, A.K., Drummond, M.L., Gonzalez, H.E., Jprgenson, K.R., Payne, S., Braunfeld, J., De Jesus, M. and Johnson, V.M. (2009) CO_2-formatics: how do proteins bind carbon dioxide? J. Chem. Inf. Model. 49, 2111–2115.
[34] Schultz, C.P., Eysel, H.H., Mantsch, H.H. and Jackson, M. (1996) Carbon dioxide in tissues, cells, and biological fluids detected by FTIR spectroscopy. J. Phys. Chem. 100, 6845–6848.
[35] Mascetti, J. and Tranquille, M. (1988) Fourier transform infrared studies of atomic Ti, V, Cr, Fe, Co., Ni, and Cu reactions with carbon dioxide in low-temperature matrices. J. Phys. Chem. 92, 2177–2184.
[36] Kazarian, S.G., Vincent, M.F., Bright, F.V., Liotta, C.L. and Eckert, C.A. (1996) Specific intermolecular interaction of carbon dioxide with polymers. J. Am. Chem. Soc. 118, 1729–1736.
[37] Roseboom, W., Blokesch, M., Böck, A. and Albracht, S.P. (2005) The biosynthetic routes for carbon monoxide and cyanide in the Ni-Fe active site of hydrogenases are different. FEBS Lett. 579, 469–472.
[38] Lenz, O., Zebger, I., Hamann, J., Hildebrandt, P. and Friedrich, B. (2007) Carbamoylphosphate serves as the source of $CN(-)$, but not of the intrinsic CO in the active site of the regulatory [NiFe]-hydrogenase from *Ralstonia eutropha*. FEBS Lett. 581, 3322–3326.